

kW/cm² VCSEL Arrays for High Power Applications

Michael Miller and Martin Grabherr

High beam qualities at high optical output powers make VCSELs attractive light sources for various applications like printing, engraving or pumping of solid state lasers. We report on mounted AlGaAs-GaAs two-dimensional VCSEL arrays of 0.123 mm² size emitting 1.4 W cw optical output power at 10 °C. The emitting wavelength of these bottom emitting VCSELs is 980 nm. The power density spatially averaged over the cleaved laser chip is as high as 1.1 kW/cm². Narrow circular far-fields below 12° FWHM allow easy focusing of the light to a spot size of less than 100 μm resulting in a power density of above 10 kW/cm². Mounting of the VCSEL array is very convenient since there is no need to take care of precise facet alignment as required for conventional edge emitting laser arrays. Simple mounting on copper heat sinks or microchannel coolers leads to inexpensive laser modules with output powers in the Watt regime. Lifetime testing for more than 7000 hours at room temperature performed at 1 A current corresponding to an output power of about 440 mW has shown a degradation rate of about 1 % per 1000 hours which is very promising for industrial applications.

1. Introduction

With the introduction of a vertical-cavity surface-emitting laser diode the cornerstone of a very promising device was laid. Main advantages of such devices include the free design of the cross-sectional area of the cavity, single longitudinal mode emission due to the very short effective resonator of about 1 μm length, transverse mode control by appropriate choice of the mesa diameter [1]. The enormous potential of single-mode devices is shown in optical data communication with data rates of 12.5 Gbit/s at bit error rates of less than 1×10^{-11} [2]. Another enormous advantage of the vertical outcoupling of the optical beam is the possibility to form two-dimensional arrays being used by many groups for highly parallel optical links [3, 4]. One can easily process neighboring devices with a spacing of 10 μm and the dimensions of an array are then practically given by the area of the wafer. Improvements of the epitaxial material, optimized processing like wet oxidation of the current aperture, improved device design and an established mounting technique for heat removal have led to VCSELs that emit optical powers of some hundreds of Milliwatts or even Watts for VCSEL arrays [5, 6]. Due to favorable beam profile, uncritical alignment tolerances for mounting, resistance against COMD (catastrophic optical mirror damage) and high reliability, VCSELs represent a dedicated light source for various fields of medium to high power applications like printing, engraving, marking, material treatment or even free space data transmission.

2. Array Fabrication

The epitaxial structure of the VCSEL devices is grown by solid source molecular beam epitaxy (MBE) on GaAs substrate and is shown schematically in Fig. 1. The p-type Bragg mirror

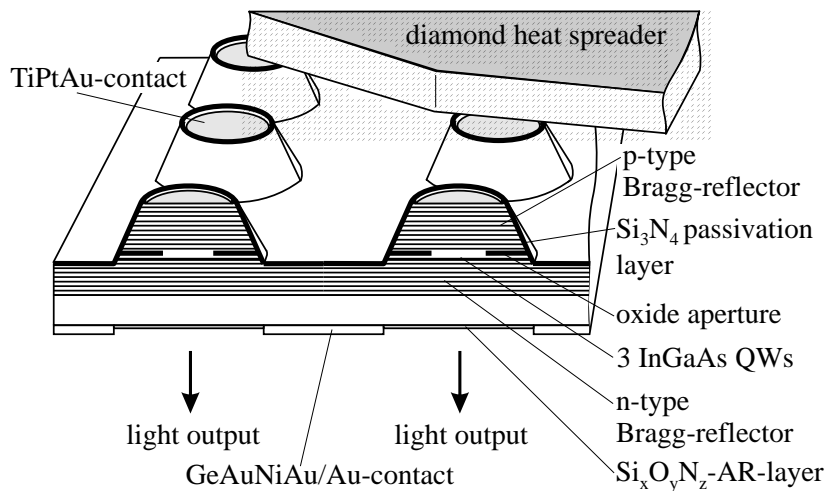


Fig. 1. Schematic drawing of a two-dimensional bottom emitting VCSEL array soldered on diamond heat spreader.

is made up by 30 pairs of $\lambda/4$ -thick AlGaAs-GaAs layers and is doped with carbon. The n-type Bragg mirror consists of 20.5 pairs of the same material and is doped with silicon. The outcoupling ratio between the upper and lower mirror is about 1:30. To minimize the dissipated power and the absorption in the resonator the doping has to be modulated between individual layers of the Bragg mirrors to reduce differential electrical resistance and light absorption. The mask design of the array consists of 19 elements in a honeycomb-like arrangement to obtain tightest packaging. The diameter of the mesas is $80\ \mu\text{m}$ and the center to center spacing of

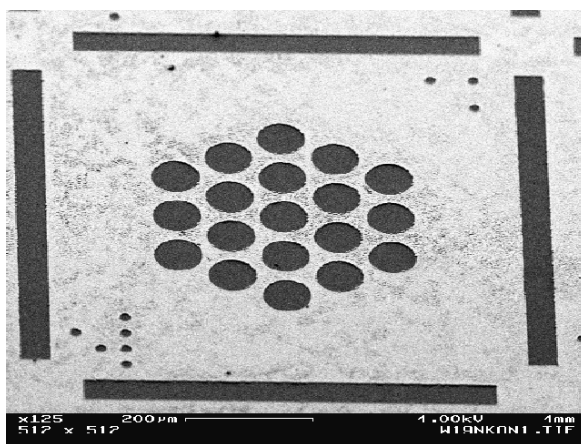


Fig. 2. N-type contact with emission windows and trenches for cleaving.

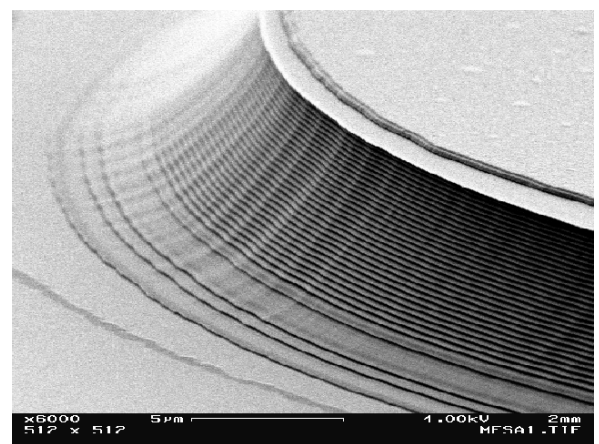


Fig. 3. Wet chemically etched mesa with p-type Bragg stack and active region.

neighboring elements is $100\ \mu\text{m}$ as shown in Fig. 2. The mesas are wet chemically etched down to the active region through the 30 nm thick AlAs layer in the p-doped region of the cladding

layer next to the active layer as can be seen in Fig. 3. To form the current aperture the AIAs is selectively oxidized to a depth of $15\ \mu\text{m}$ resulting in an active diameter of $50\ \mu\text{m}$ for each device in the array. After thinning and polishing the substrate to a thickness of less than $200\ \mu\text{m}$ an anti-reflection (AR) coating consisting of Si_xN_y is deposited on the back side of the substrate using a PECVD system. Subsequently, the emission windows are protected with photoresist and the surrounding area is etched with CAIBE or RIE. On the etched region an n-type GeAuNiAu contact is evaporated and lift-off is used to open the emission windows. On top of the mesas a full p-type TiPtAu contact is evaporated. As the final step a $1\ \mu\text{m}$ thick Au layer is electroplated on the n-type metallization. Fig. 2 shows the emission windows and the trenches for cleaving the array. After processing, the basic characteristics of the devices are recorded on wafer before cleaving.

3. Basic Characteristics

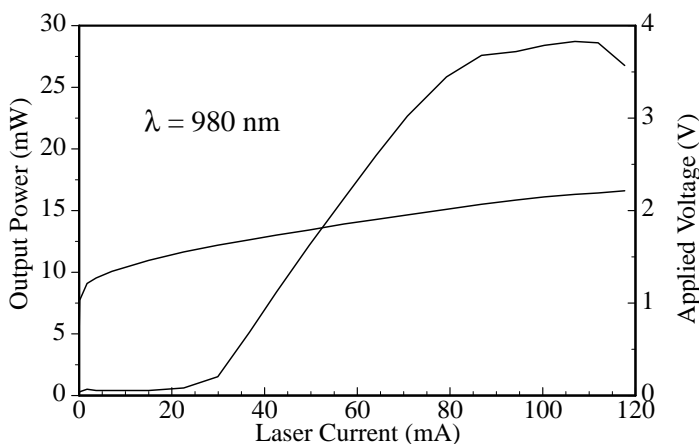


Fig. 4. Typical output characteristics of a single device with an active diameter of $50\ \mu\text{m}$.

Fig. 4 presents the typical output characteristics for a device with an active diameter of $50\ \mu\text{m}$. The basic characteristics of this VCSEL are the V-I-behavior to determine kink voltage of $1.4\ \text{V}$, threshold voltage of $1.6\ \text{V}$ and differential resistance of $7.5\ \Omega$ in the linear region. Also the L-I-behavior in the unmounted state for a single device in the array is very important to get information about the maximum output power which is about $30\ \text{mW}$ for this non heat sunk device. The threshold current can be read from the graph to be about $27\ \text{mA}$. The differential quantum efficiency of $43\ \%$ is determined from the slope in the linear region of the output power curve. From the known area of the active region the threshold current density of $1.38\ \text{kA}/\text{cm}^2$ is obtained. The combination of V-I and L-I-behavior results in the conversion efficiency by dividing the optical output power by the electrical input power which reaches a maximum of about $18\ \%$ for unmounted devices. The output characteristics of all 19 single devices of the array have to be extremely homogeneous because after mounting all devices are driven in parallel and current crowding in an element may destroy it. A very important factor for device performance is the thermal resistance since the optical output power strongly depends on the internal heating

resulting in thermal roll-over of the L-I-characteristic. The thermal resistance

$$R_{th} = \frac{\Delta T_{hs}}{\Delta P_{diss}} = \frac{(\Delta\lambda/\Delta P_{diss})}{(\Delta\lambda/\Delta T_{hs})} \quad (1)$$

defined by the ratio of temperature rise ΔT_{hs} due to the dissipated electrical power ΔP_{diss} can be obtained from the redshift $\Delta\lambda$ of the emitted wavelength of an individual mode due to increased dissipated power at constant heat sink temperature and the wavelength shift due to altered heat sink temperature at constant dissipated power. To obtain higher optical output power an improved mounting technique for heat removal is required in particular if several devices are driven in parallel. Due to the outcoupling of the light through the substrate the wavelength

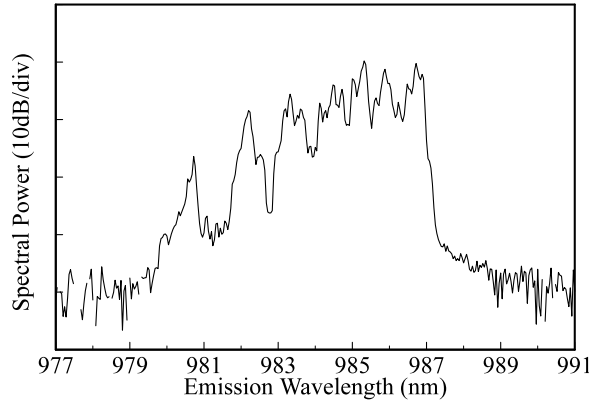


Fig. 5. Emission spectrum of the VCSEL array at a current of 2 A.

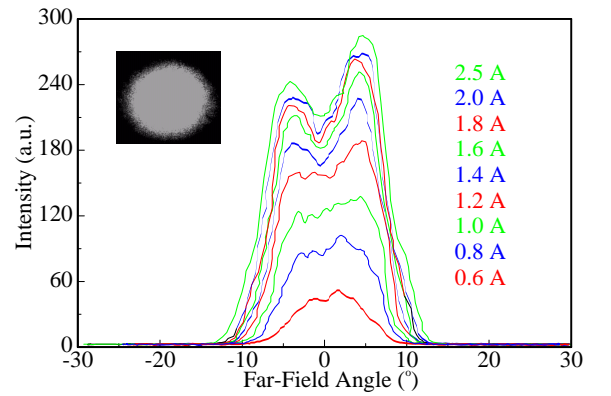


Fig. 6. Far-field pattern and cross sections at different currents.

limited to above 900 nm to avoid fundamental absorption in the substrate. The spectrum of the VCSEL array shown in Fig. 5 is centered at 984 nm. The 10 dB down span of the emitted spectrum is about 5 nm. Two factors are responsible for the spectral broadening namely the strong multi-mode emission behavior of each device in the array and the slight layer thickness variation due to non optimized MBE growth resulting in a wavelength shift of about 3.5 nm across the array of 450 μm width.

The cross sectional far-field angle in Fig. 6 is recorded by a photo diode which is rotated over the semi-circle of the emission direction. The inset shows the circular-symmetric far-field pattern on a focusing screen. For low driving currents the beam shape can be described by a Gaussian profile whereas at higher currents a doughnut-like profile occurs. For all driving currents FWHM of the far-field angle is below 12° which is very favorable for focusing or collimating optics because astigmatism is much weaker as compared to edge emitting lasers.

4. Mounted Arrays

Thermal behavior has a strong influence on the optical output characteristics because thermal rollover limits maximum power. From experimental results we know that the point of thermal

turn-off occurs at an internal temperature of about 200°C [7]. If one can reduce heat generation by lower electrical series resistances or suppress temperature rise by increased thermal conductivity the output power will increase accordingly. The specific thermal conductivity of

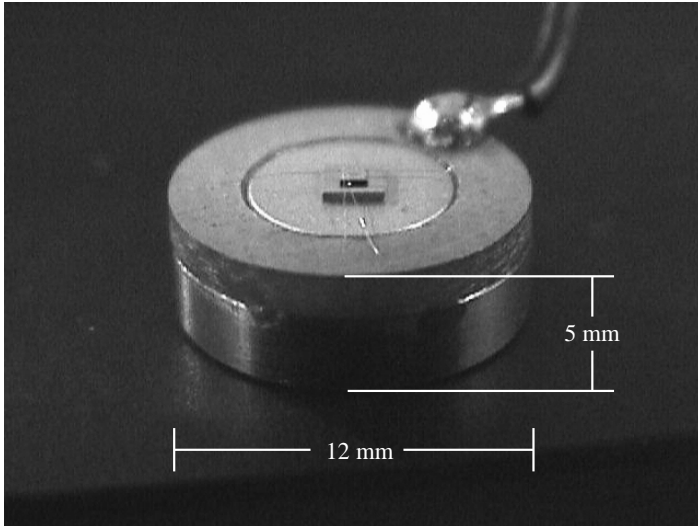


Fig. 7. Mounted VCSEL-array on metallized diamond and copper heat sink.

GaAs is about $\lambda_{GaAs} = 44 \text{ W/K}\cdot\text{m}$. Heat dissipation can be strongly increased by soldering the chip up-side down on a diamond heat spreader ($\lambda_{Dia} \geq 1000 \text{ W/K}\cdot\text{m}$) or a copper heat sink ($\lambda_{Co} \approx 400 \text{ W/K}\cdot\text{m}$). For mounting the array is first cleaved with the dimensions of $800 \times 800 \mu\text{m}^2$ and soldered with eutectic $\text{Au}_{80}\text{Sn}_{20}$ on a metallized diamond of $2 \times 2 \text{ mm}^2$ area as can be seen in Fig. 7. This module is then soldered on a copper heat sink using eutectic $\text{Au}_{80}\text{Sn}_{20}$. Both solderings are realized in only one heating-up step at a temperature of about 290°C. The copper heat sink has a diameter of 12 mm and a height of 5 mm. The thermal capacitance of this small volume is not big enough to drive the array satisfactory in cw mode. For this reason a thread is drilled in the backside of the copper to mount this heat sink easily on a bigger heat sink with higher thermal capacitance using a screw. The heat sink provides the common p-contact for all devices in the array so that all elements are operated in parallel. After mounting the array is bonded on the galvanic n-contact with bond wires to an insulated

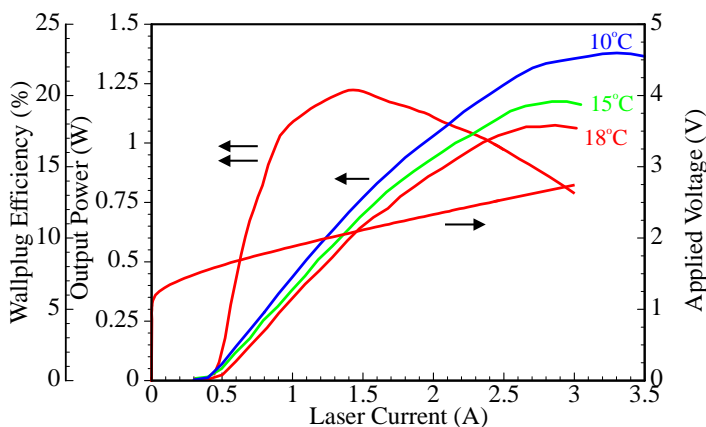


Fig. 8. Output characteristics of a mounted VCSEL-array at different heat sink temperatures.

copper plate for current supply. With an expected driving current of about 3 to 4 A, eight wires with a diameter of 30 μm were bonded to guarantee a low resistance electrical connection. The module can be driven as a passive heat sink or connected to a Peltier element for active cooling. Fig. 8 shows the output characteristics of a mounted VCSEL array consisting of 19 elements with an active diameter of 50 μm for different heat sink temperatures. The threshold current varies from 480 mA at 18°C to 400 mA at 10°C indicating a slight detuning of gain and cavity resonance caused by internal heating due to the dissipated power at threshold. The maximum output power at room temperature of 1.08 Watt increases up to 1.4 Watt at 10°C. If we take a chip size close to the honeycomb-like arrangement of the lasers into account the spatially averaged power density at 1.4 Watt is as high as 1.15 kW/cm². By reducing the diameter of the focal spot by a factor of 3 with a lens the power density increases above 10 kW/cm² which is promising for many applications. The differential resistance is 0.48 Ω which is slightly larger

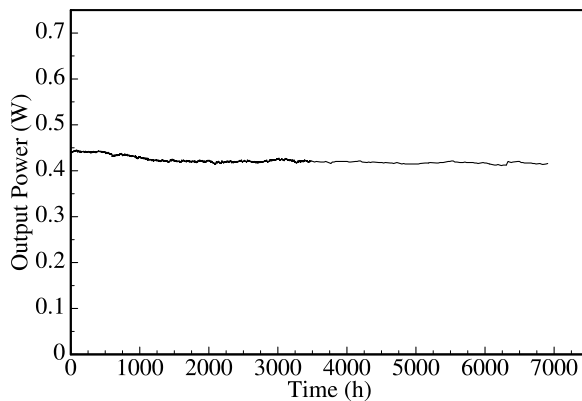


Fig. 9. Lifetime testing of a VCSEL-array at a current of 1 A and a corresponding output power of about 440 mW.

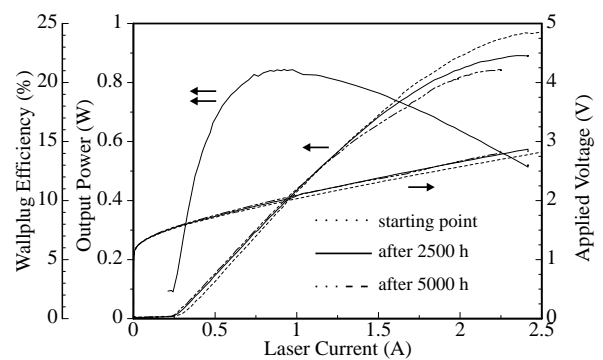


Fig. 10. Output characteristics of the array at the beginning, after 2500 hours and after 5000 hours of duty.

than that of 19 lasers with 7.5 Ω driven in parallel. The discrepancy is due to additional ohmic losses in the bond and solder connections. The maximum conversion efficiency exceeds 20 % for all temperatures at 3 times threshold and the maximum output power is reached at 6 to 7 times threshold. The differential conversion efficiency is larger than 50 % but there is still some place for improvements by optimizing the mirror reflectivities and minimizing the absorption by changing the doping profile. Fig. 9 illustrates lifetime testing of an array driven at a current of 1 A corresponding to an optical output power of 440 mW. The array mounted on a microchannel cooler fabricated by the ILT Fraunhofer Institut at Aachen is operated for more than 7000 hours at room temperature. The total degradation rate is about 7 % corresponding to 1 % per 1000 hours. The slight variation of output power over short periods of time can be explained by fluctuations of the water temperature. The output characteristics at the beginning of the test, at 2500 hours, and at 5000 hours are given in Fig. 10. The minor decrease of the threshold current may be caused by burn-in effects.

5. Conclusion

We have fabricated and characterized high-power VCSEL arrays consisting of 19 single devices with active diameters of 50 μm emitting at a wavelength of 980 nm. Maximum output power is 1.08 Watt for cw operation at room temperature and 1.4 Watt at a heat sink temperature of 10°C. Simple focusing to a spot size of about 100 μm diameter yields cw power densities in excess of 10 kW/cm². Applications for this power regime are marking of foils, joining or cutting of plastics and pumping of solid state lasers. In the future, we plan to design new heat sinks for larger arrays consisting of about 50 to 100 single devices. With a target optical power of about 10 Watts we have to deal with approximately 100 Watts of dissipated power at a soldered area of about 0.25 to 0.5 mm².

References

- [1] C. Jung, R. Jäger, M. Grabherr, P. Schnitzer, R. Michalzik, B. Weigl, S. Müller, and K. J. Ebeling, "4.8 mW singlemode oxide confined top-surface emitting vertical-cavity laser diodes," *Electron. Lett.* **33**, pp. 1790–1791, 1997.
- [2] F. Mederer, C. Jung, R. Jäger, M. Kicherer, R. Michalzik, P. Schnitzer, D. Wiedenmann, and K. Ebeling, "12.5 Gbit/s data rate fiber transmission using single-mode selectively oxidized GaAs VCSEL at $\lambda = 850$ nm," in *LEOS Annual Meeting 1999*, vol. 2, pp. 697–698, (San Francisco, USA), Nov. 1999.
- [3] H. Karstensen, L. Melchior, V. Plickert, K. Drögemüller, J. Blanck, T. Wipijewski, H.-D. Wolf, J. Wieland, G. Jeiter, R. Dal'Ara, and M. Blaser, "Parallel optical link (PAROLI) for multichannel gigabit rate interconnects," in *48th Electron. Comp. and Technol. Conf., ECTC'98*, pp. 747–754, (Seattle, WA, USA), May 1998.
- [4] D. Wiedenmann, R. King, C. Jung, R. Jäger, R. Michalzik, P. Schnitzer, M. Kicherer, and K. J. Ebeling, "Design and Analysis of Single-Mode Oxidized VCSEL's for High-Speed Optical Interconnects," *IEEE J. Select. Topics Quantum Electron.* **5**, pp. 503–511, 1999.
- [5] M. Grabherr, M. Miller, R. Jäger, R. Michalzik, U. Martin, H. Unold, and K. J. Ebeling, "High-Power VCSEL's: Single Devices and Densely Packed 2-D-Arrays," *IEEE J. Select. Topics Quantum Electron.* **5**, pp. 495–502, 1999.
- [6] D. Francis, H. Chen, W. Yuen, G. Li, and C. Chang-Hasnain, "Monolithic 2D-VCSEL array with >2W CW output power," in *IEEE Int. Semiconductor Laser Conf. (ISLC)*, pp. 99–100, (Nara, Japan), Oct. 1998.
- [7] B. Weigl, M. Grabherr, C. Jung, R. Jäger, G. Reiner, R. Michalzik, D. Sowada, and K. J. Ebeling, "High-Performance Oxide-Confined GaAs VCSEL's," *IEEE J. Select. Topics Quantum Electron.* **3**, pp. 409–415, 1997.